# Water-induced polaron formation at the pentacene surface: Quantum mechanical molecular mechanics simulations

Tobias Cramer,[1] Thomas Steinbrecher,[2] Thorsten Koslowski,[3] David A. Case,[2] Fabio Biscarini,[4] and Francesco Zerbetto[1]
[1]*Dipartimento di Chimica "G. Ciamician," Università di Bologna, Via F. Selmi 2, 40126 Bologna, Italy*
[2]*BioMaPS Institute and Department of Chemistry & Chemical Biology, Rutgers University, 610 Taylor Road, Piscataway, New Jersey 08854-8087, USA*
[3]*Institute for Physical Chemistry, University of Freiburg, Albertstrasse 23a, 79104 Freiburg, Germany*
[4]*CNR-Institute for the Study of Nanostructured Materials, Via Gobetti 101, 40129 Bologna, Italy*
(Received 12 November 2008; revised manuscript received 16 March 2009; published 22 April 2009)

Water is an omnipresent polar impurity that is expected to be the origin of many electric degradation phenomena observed in organic semiconductors. Here, we describe a microscopic model for polaron formation in the outermost layer of a pentacene crystal due to the polarization of a nearby water layer. The efficient coupling of a classical force field that describes the liquid with a tight-binding model that represents the $\pi$ system of the organic layer permits the calculation of nanosecond length trajectories. The model predicts that the reorientation of water dipoles stabilizes positive charge carriers on average by 0.6 eV and thus leads to a polaron trap state at the liquid interface. Thermal fluctuations of the water molecules provoke two-dimensional diffusive hopping of the charge carrier parallel to the interface with mobilities of up to 0.6 $cm^2\ s^{-1}\ V^{-1}$ and lead to an amorphous broadening of the valence-band tail. As a consequence, water-filled nanocavities act as trapping sites in pentacene transistors. Instead, a complete wetting of the organic film is expected to result in fast thermally activated hopping transport. Polaron trapping is thus not expected to be a limiting factor for transistor-based sensors that operate under water.

DOI: 10.1103/PhysRevB.79.155316 PACS number(s): 73.40.−c, 85.65.+h, 73.20.Fz, 73.61.Ph

## I. INTRODUCTION

One of the main hindrances to the application of organic semiconductors in low cost electronics or sensing applications is their limited operational capacity under ambient conditions. Mechanisms of degradation include redox reactions involving water and oxygen,[1] structural instabilities[2] of the organic film, or charge-carrier scattering and trapping due to polar impurities.[3] While the first two mechanisms can be controlled via the redox potential of the organic semiconductor and its adhesion to the solid support, little is known about how polarizable species, such as water, affect the charge-carrier transport due to direct electrostatic interactions. A detailed microscopic understanding of this effect is crucial in the field of biosensors based on organic electronics where the basic idea is that interactions between an aqueous protein solution and charge carriers in the semiconducting film lead to a specific change in conductive properties and thus induce a signal.[4] In general, the inhomogeneous electric field created by polar impurities introduces disorder in the electronic structure of the semiconductor and reduces mobility via carrier scattering.[5] This static picture of the role of impurities is overcome when polarization and thermal fluctuations are considered. The effects should be especially important for water where the rearrangement of dipoles might introduce strong polaronic charge localization: a phenomenon that has not yet been taken into account for the explanation of water-related degradation of organic semiconductors.

In this study, we focus on the effect of water on charge transfer through ultrathin layers of pentacene, which is typically measured in a thin-film transistor (TFT) setup. Pentacene represents one of the most intensely studied molecules as the active organic layer in TFTs. Upon high-vacuum sublimation, pentacene molecules form highly ordered layered films where molecules exhibit strong $\pi$ stacking in-plane interactions (viz., along the directions parallel to the film) and weaker interlayer interactions. This leads to a large band dispersion in plane and consequently high carrier mobilities in the range of 1 $cm^2\ V^{-1}\ s^{-1}$ for polycrystalline TFTs (Ref. 6) and 10–100 $cm^2\ V^{-1}\ s^{-1}$ in highly purified single crystals.[7] Recent experimental results demonstrated how water influences the device performance.[8,9] Pentacene TFTs were exposed to controlled amounts of humidity and a decrease in conductivity was observed on a long time scale (hours). The findings could be partially explained by introducing a water-related trap state at an energy of 0.43 eV. The slow trapping dynamics were rationalized by the diffusion of water into the hydrophobic film. *Ab initio* calculations have provided a microscopic model for this defect state in which a single water molecule is intercalated into the pentacene film.[10]

As an alternative to a single water molecule impurity, one has to consider water-filled nanocavities that may exist either due to fluctuations of the pentacene surface or due to defects at the dielectric interface.[8,11,12] Atomic force microscopy (AFM) reveals that the multiple stacking of monolayer terraces leads to topographical fluctuations at the surface of ultrathin pentacene films.[13] Traces of humidity are likely to condense in the cavities formed by the topological minima [see Fig. 1(C) box a]. In addition, water layers can be present at the interface between the dielectric and the pentacene film as evidenced by x-ray experiments for a silicon dioxide dielectric [see Fig. 1(C) box b].[11] In both cases, strongly polarizable water is close to the lowest pentacene layers where the charge accumulation occurs.[14,15] As a consequence, water-filled cavities may be responsible for the experimentally observed decrease in mobility under humidity.[11] Freezing of water-filled nanocavities in thin films was also proposed as a mechanism for the increased bias-stress stability

 

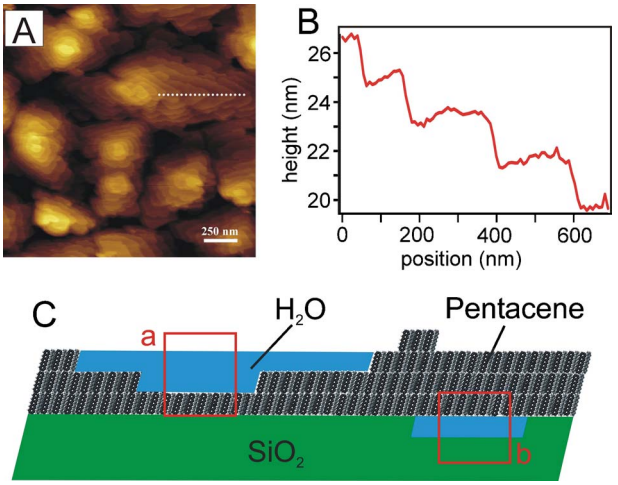


FIG. 1. (Color online) Possible water-filled cavities in pentacene films. (a) Height profile of an ultrathin pentacene film as obtained by AFM measurements and (b) according cross section at the indicated position [dotted line in (a)]. (c) Schematic cross section of a film with possible water-filled cavities. The parts of the film that correspond to the simulation cell are marked by boxes.

at lower temperatures.[8,12] Remarkably, recent experiments demonstrated that TFTs based on pentacene[14] or other organic semiconductors[16] can be operated even fully immersed in water as long as source-drain voltage is kept low to prevent electrolysis. In this paper, we derive a theoretical model that accounts for the influence of water on organic semiconductors. Our conclusions are based on the simulation of a pentacene monolayer that is in contact with a water layer. The simulation box was chosen to represent the two cases where water is in closest contact to the lowest conducting sheets of a pentacene thin film (see Fig. 1) and where the polaron trapping seems likely to influence the device performance.

The influence of dielectric polarization on charge-carrier mobility was recently studied in organic field-effect transistor (OFETs).[17] As the majority of charge carriers moves close to the surface of the organic semiconductor, polarization does not only affect the charge carrying phase but may also extend into the nearby gate dielectric. By changing the dielectric and its polarizability systematically, the researchers proved the formation of small polarons.[17] With increasing permittivity, the charge carrier is more strongly coupled to nuclear displacements in the dielectric. As a result, a decrease in mobility and a shift of its temperature dependence from a metallic-like regime to thermally activated behavior were observed. Since a water "impurity" layer has an even higher permittivity than the gate insulators investigated in that work, the polaron formation in the vicinity of water-filled cavities can be anticipated.

The coupling of charge carriers to the nuclear motion leads to the charge localization into polaron states, a process that can be well described by model Hamiltonians.[18] One distinguishes typically between nuclear motions that take place on the molecular parts where the charge is localized (inner-sphere reorganization) and motions in the surrounding (outer-sphere reorganization).[19] For the former, one has to introduce a direct electron-phonon coupling, for example, in the form of the Su-Schrieffer-Heeger model.[20] The latter is often described by the approximation of an effective polarizable continuum that surrounds the polaron and can be cast into Hubbard-model-type Hamiltonians.[21] Rearrangements in both types of nuclear coordinates reduce the energy of the charge carrier by the polaron binding energy $E_P$. Its value enters as an effective parameter in the model-Hamiltonian approaches. In the absence of disorder effects, the localization of charge carriers is then controlled by the ratio of the polaron binding energy $E_P$ and the transfer integral $V_{DA}$ between donor and acceptor states. In the limit of strong coupling ($E_P \gg V_{DA}$), the polaron is localized on a single lattice site and the transfer is described by thermally activated hopping on the adiabatic energy landscape.

In contrast to the model-Hamiltonian approach, atomistic models for the polaron formation in organic semiconductors are sparse since the coupling between the numerous electronic and nuclear degrees of freedom requires a tremendous computational effort.[22] In addition, the geometry at the surface of the organic crystal or film which is in contact with the impurity is not known. Nevertheless, due to their possible importance for device degradation, there is a need for microscopic understanding of polaronic trap formation. For the case of pentacene in contact with water, we derive such a model in the present study. The essential simplification comes from the division of the system into classical nuclear degrees of freedom that belong to the water molecules [the molecular mechanics (MM) part] and the electronic degrees of freedom that are represented by the $\pi$-orbital system of the pentacene layer [the quantum mechanical (QM) part]. The strong polaron coupling energy justifies the adiabatic approximation in our study and the nuclear coordinates can be propagated in time considering only ground-state forces. As a result, we do not only obtain values for polaron binding energy and localization measures but also dynamic properties such as the time scale for water-induced polaron formation and diffusion.

## II. THEORY AND METHODS

In our simulation, the pentacene film is constructed according to the single-crystal structure published by Mattheus *et al.*[23] Although in pentacene thin films several different unit-cell dimensions were observed we neglect the effects of polymorphism in this work. A detailed comparison of band structures and coherent charge transfer in different polymorphs was given by Troisi *et al.*[24] However, the observed changes in electronic couplings are small and it is not expected that they have a strong impact on the incoherent charge-transfer mechanism that is studied here. To obtain the film geometry, we multiply the crystal cell four times in the $a$ direction and three times in the $b$ direction. Altogether the film then consists of 24 pentacene molecules [see Fig. 2(b)]. As a simulation box, we use a supercell of the dimensions $a=24.96$ Å, $b=22.91$ Å, and $c=100.00$ Å and the angles $a$, $b=90.00°$, and $c=84.68°$. We apply the minimum image convention. The large extension in the $c$ direction inhibits the interaction of the film with itself. On one side of the penta-

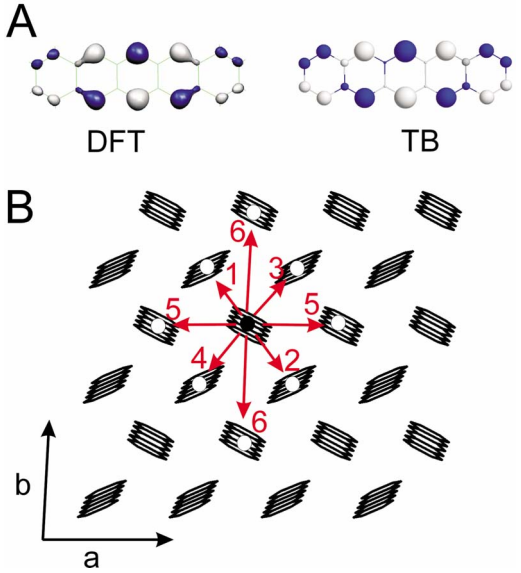


FIG. 2. (Color online) (a) Visualization of the highest-occupied molecular orbital of pentacene: comparison between density-functional theory (DFT) and parametrized tight-binding (TB) calculation. (b) Geometry of the simulation box representing the pentacene monolayer. The nearest-neighbor hoppings are indicated.

cene film, we then introduce the water layer composed of 548 molecules in random bulk-water conformation as initial geometry.

The classical MMs part of our simulation includes the water film whose properties are described by the standard SPC/E water model (a reparametrized version of the SPC or *simple point charge* water model).[25] This model was chosen for its simplicity and good agreement with experimental values for the surface tension and permittivity,[26] which are crucial for the studied phenomenon. Lennard-Jones-type van der Waals interactions between water molecules and the pentacene film are evaluated according to the generalized Amber force field.[27] The electrostatic interaction with the quantum system is described below.

The QM part contains the pentacene film. Its electronic structure is calculated in the one-electron tight-binding approximation. The corresponding Hamiltonian has the form

$$\hat{H} = \sum_i (\varepsilon_i + \phi_i) a_i^\dagger a_i + \sum_{ij}{}' V_{ij} a_i^\dagger a_j. \tag{1}$$

Creation $a_i^\dagger$ and annihilation $a_i$ operators act on a basis of $p_z$ atomic orbitals (AOs) of carbon atoms ($N=24\times22$) which is assumed to be orthogonal. $\varepsilon_i$ denotes the atomic site energies, which are here defined as $\varepsilon_{\mathrm{CH}}$ for hydrogen-bonded carbon atoms. For the other carbon atoms in pentacene, we introduce the parameter $\varepsilon_{\mathrm{CC}}$. The electrostatic interactions with the MM part of the simulation enter via the site potential $\phi_i$ (see below). Electronic coupling between the atomic orbitals is represented by the nondiagonal elements $V_{ij}$. We introduce two different parameters for intramolecular couplings: $V_{\mathrm{CC}}$ for $\pi$ bonds between carbon atoms that are not bound to hydrogen and $V_{\mathrm{CCH}}$ for the remaining $\pi$ bonds in the pentacene molecule.

Parametrization of the atomic site energies $\varepsilon_{\mathrm{CC}}$, $\varepsilon_{\mathrm{CH}}$, and the two intramolecular couplings $V_{\mathrm{CC}}$ and $V_{\mathrm{CCH}}$ is based on a comparison to a DFT calculation on a single pentacene molecule at the Becke, three-parameter, Lee-Yang-Parr (B3LYP) level with a split valence basis set ($6-31G^{**}$), where the root-mean-square (RMS) deviation between the DFT and TB $\pi$ orbital energy levels has been minimized. By considering only the six $\pi$-orbital states closest to the highest-occupied molecular orbital (HOMO)-lowest-unoccupied molecular orbital(LUMO) gap, the RMS value amounts to 0.053 eV. The final parameter values obtained are $\varepsilon_{\mathrm{CH}}=-3.37$ eV, $\varepsilon_{\mathrm{CC}}=-3.32$ eV, $V_{\mathrm{CC}}=-1.77$ eV, and $V_{\mathrm{CCH}}=-4.23$ eV. An assessment of the quality of the parametrization beyond the RMS value is possible. As the hole is created in the HOMO of the TB model, this molecular orbital should exhibit a close similarity to its DFT counterpart. In Fig. 2(a) we display a graphical representation of the *ab initio* HOMO utilizing the MOLEKEL program and the corresponding TB atomic-orbital coefficients. We note that not only the sign of the atomic-orbital contributions to the HOMO and its nodal structure are well represented but the numerical values of the TB HOMO also provide a very good description of the highest-occupied DFT orbital.

The long-range intermolecular electronic couplings between $p_z$ orbitals are evaluated according to Slater-Koster rules[28] following a procedure already described by two of the authors.[29] We also adopt the same parametrization of the distance dependence of the electronic overlap.[29] The validity of this parametrization for pentacene can be assessed by a comparison with the experimental density of states [(DOS) see below)]. Matrix elements for the intermolecular coupling were evaluated at the start of the simulation and then frozen. In this way, we neglect nondiagonal disorder effects due to the thermal motion of pentacene molecules. Although recent calculations[30] have suggested their possible impact on transfer mechanism, we justify our simplification by the large strength of the diagonal disorder introduced by the water and the consequent localization of electronic states (see below). Due to our assumption of a stiff pentacene layer and the neglect of the underlying $\sigma$ electrons, we do not include the nuclear and electronic polarization of neutral pentacene molecules which affect the inner-sphere reorganization in charge transfer. However, it was shown by photoelectron spectroscopy and theoretical modeling that the inner-sphere reorganization in pentacene is rather small $E_P^0=\lambda/2=0.05$ eV, where $\lambda$ is the Marcus reorganization energy.[31]

In this study, the division between the QM and the MM part is defined by the phase boundary between water and pentacene and does not include any cuts through covalent bonds. For the coupling between the two regions, we just have to evaluate the electrostatic site potentials $\phi_i$ acting on the AO basis and the charge distribution of the positive hole that exerts an electrostatic force on water molecules. For the former we apply the Coulomb potential,

$$\phi_i = -\frac{e^2}{4\pi\varepsilon_0} \sum_{j\in MM} \frac{q_j}{r_{ij}}. \tag{2}$$

Here $q_j$ denote the classical point charges of the SPCE water model.[32] The long-range part of Eq. (2) is calculated via

particle mesh Ewald summation.[33] As the total dipole moment of the simulation cell is small, we neglect a correction that accounts for the slab geometry. To obtain the charge distribution $\{q_i\}_{\mathrm{QM}}$ of the positive hole on the atomic sites $i$ of the pentacene film, we diagonalize the tight-binding matrix. Here the adiabatic (Born-Oppenheimer) approximation is justified because the polaron makes only short hopping steps between neighboring sites whose electronic coupling is sufficiently large. As the hole resides in the highest-occupied eigenstate of the system, we calculate the point charges $q_i$ from the atomic-orbital coefficients $c_{i,N/2}$,

$$q_i = c_{i,N/2}^2 \quad \text{for} \quad i \in \mathrm{QM}. \tag{3}$$

Following Hellman-Feynman theorem, forces between the MM and the QM part arise only due to electrostatic interactions between the hole charge distribution $\{q_i\}_{\mathrm{QM}}$ and the SPCE water multipoles. We calculate them in a second Ewald summation that now includes the QM charges $\{q_i\}$ and the corresponding negative background charge.

Simulations were performed with a modified version of the AMBER10 program,[34] with additional modifications to describe the QM system. Initial geometries were subjected to a 100 steps steepest-descent minimization in the absence of a positive hole. Molecular-dynamics (MD) trajectories were then calculated with a time step of 2 fs in the *NVT* ensemble using the SHAKE algorithm[35] to constrain bonds involving hydrogen. Temperature equilibration to 298 K was performed by coupling to a Berendsen-type thermostat with a coupling constant of 0.2 ps for 2.5 ps in the presence of the positive hole. Productions runs were conducted for at least 400 ps with a coupling of 5.0 ps to the thermostat.

In order to characterize the localization of electronic eigenstates $\alpha$, we calculate the radius of gyration $R_G$ in which we use the electronic probability of occurrence $c_{i,\alpha}^2$ instead of masses

$$R_G = \left[ \frac{1}{N} \sum_{i \in \mathrm{QM}} c_{i,\alpha}^2 (\vec{x}_i - \vec{s}_\alpha)^2 \right]^{1/2}. \tag{4}$$

The localization center of the eigenstate is denoted by $\vec{s}_\alpha$. Taking the periodic boundary condition into account, it is defined to be the point at which Eq. (4) reaches its minimum value. To analyze the effects of the anisotropy of the pentacene film, we calculated also the spatial extension of the eigenstate in the three pentacene unit-cell directions $a,b,c$ and denote them as $R_{G,a}$, $R_{G,b}$, and $R_{G,c}$.

## III. RESULTS

Even in the absence of a positive charge (electron hole), the unpolarized water layer has a profound effect on the electronic structure of the pentacene film. Figure 3 compares the density of $\pi$-orbital states (DOS) in the simulation box in the absence and in the presence of the water layer. In the undisturbed pentacene film, we observe a band gap of 1.93 eV and the width of the valence band amounts to 0.30 eV. The values are in reasonable agreement with the band gap of 1.8 eV and the maximum band dispersion of 0.33+/−0.04 eV as obtained by photoelectron spectroscopy[36] or first-principles

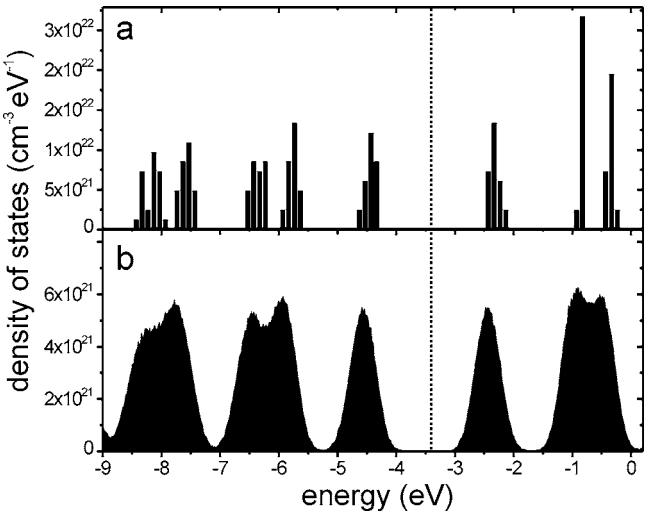


FIG. 3. Density of states in the neutral pentacene simulation box. (a) In the absence of water. (b) In contact with the water film and averaged over a 200 ps trajectory. The dashed line marks the Fermi level.

calculations.[37] In contrast, the DOS of the film in contact with water shows a significant broadening. The width of the valence band now amounts to 0.55 eV and it shows amorphous band tails. The origin of the effect is in the diagonal disorder introduced in the tight-binding matrix by the electrostatic coupling to the water dipoles. The fluctuation of the onsite potentials follows a Gaussian distribution with a standard deviation of $\sigma_\phi = 0.19$ eV.[38] As a consequence, the contact to the dielectric layer leads to a symmetric level broadening but does not change the Fermi level of the interfacial electronic states ($\Delta\varepsilon_F < 0.03$ eV).[39]

Amorphous band tails of the pentacene valence band have been deduced from photoconductivity measurements and temperature-dependent FET conductivity measurements.[40] In agreement with the Urbach rule,[41] the tails have been fitted by an exponential decay of the form $N(E) = N_0 \exp(-\beta|E|)$. While values for $N_0$ depend strongly on the crystal and device processing and vary by orders of magnitude, the decay parameter $\beta$ lies in the range of 5–25 eV$^{-1}$. The same type of analysis for the calculated DOS yields $N_0 = 3.4 \times 10^{21}$ cm$^{-2}$ eV$^{-1}$ and $\beta = 9.0$ eV$^{-1}$. The calculated $N_0$ can be regarded as an upper limit. In the simulation, the DOS is calculated only for a layer in contact with water while in experiments the probed part of the film consists of a mix of undisturbed pentacene layers and layers in contact with water-filled nanocavities. In contrast to $N_0$ the decay parameter $\beta$ is independent of the amount of water cavities. Especially the good agreement with data deduced from pentacene single-crystal FET measurements ($\beta = 9.3$ eV$^{-1}$) (Ref. 40) suggests interfacial water cavities as a possible explanation for the observed amorphous band tails.

The localization properties of the electronic states close to the band gap strongly influence the conduction mechanism through the perturbed film.[42] In our calculation, we find that the average spatial extension of the highest-occupied electronic state is in the range of the lattice spacing. Its average radius of gyration amounts to $\langle R_G \rangle = 5.8$ Å (see Table I). As

TABLE I. Average spatial extension $\langle R_G \rangle$ of the highest-occupied electronic state in a pentacene molecule, a pentacene film in contact with water, and a charged pentacene film in contact with water. $a$, $b$, and $c$ denote the directions of the pentacene unit cell, where $c$ points in the direction of the molecular axis.

| | Charge | $\langle \boldsymbol{R}_G \rangle$ (Å) | $\langle \boldsymbol{R}_{G,a} \rangle$ (Å) | $\langle \boldsymbol{R}_{G,b} \rangle$ (Å) | $\langle R_{G,c} \rangle$ (Å) |
|---|---|---|---|---|---|
| Molecule, vacuum | 0 | 3.8 | | | 3.3 |
| film, water | 0 | 5.8 | 3.3 | 3.7 | 3.3 |
| film, water | +1 | 5.3 | 3.0 | 3.2 | 3.3 |

the strength of the diagonal disorder in the tight-binding matrix $\sigma$ exceeds the bandwidth, the system is in the regime of strong Anderson localization.[43] At this point we can already deduce from the calculations of the neutral system that in the presence of water, charge transport has to occur via thermally activated hopping between localized states.

In addition to polar disorder, the polarization of nuclear degrees of freedom leads to further charge localization and to the formation of polaronic states. In our simulations, we study this effect by removing an electron from the pentacene film and thereby introducing a hole in the simulation cell. The positive hole exerts an electrostatic force on the water multipoles, the polarization of which in turn influences the hole localization. We generated a trajectory for the coupled QM-MM system by numerical propagation according to standard MD techniques (updating the QM forces at every time step). The *NVT* ensemble is maintained due to the coupling to a thermal bath. The algorithm is efficient enough to allow us to compute QM-MM trajectories of several nanoseconds length on a single processor in approximately 80 h. Figure 4 gives a graphical representation of a snapshot obtained from a typical simulation run. The charge distribution

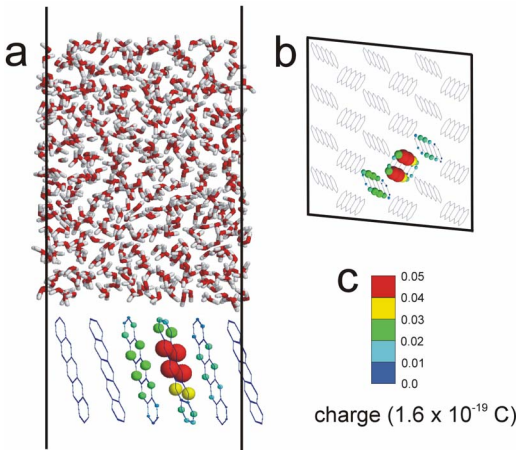


FIG. 4. (Color online) Visualization of the polaron formation due to the presence of a water film. Water molecules are shown as stick models. Pentacene molecules are drawn as wire frames, omitting hydrogens. The size and the color of the spheres represent the partial charge of the carbon atoms. (a) Cross section through the pentacene/water film. (b) Top view on the pentacene film omitting water. (c) Color coding scheme. Black lines represent the simulation cell.

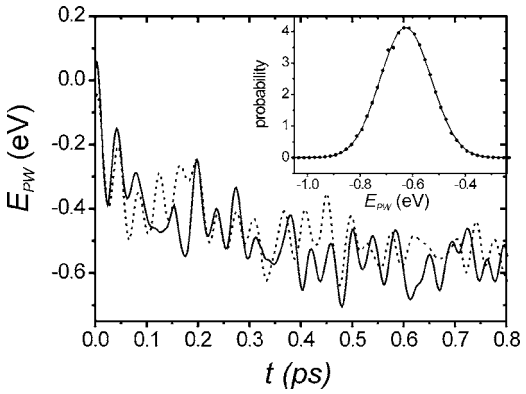


FIG. 5. Decay of the polaron binding energy $E_{\mathrm{PW}}$ due to reorganization of water molecules after injection of the positive charge into the pentacene layer at $t=0$. The solid and the dashed lines represent two trajectories with different water initial configuration. Inset: distribution of $E_{\mathrm{PW}}$ at equilibrium.

of the positive hole is visualized in a color-coded fashion. In this snapshot, the major part of the charge is located on three pentacene molecules. The center of the polaron is slightly shifted along the pentacene molecular axis toward the stabilizing water layer. Below, we describe in greater detail those polaron properties which are relevant for the device physics of a pentacene organic thin-film transistor (OTFT) in contact with water. Both the energetic stabilization and the time scale of the polaronic trap formation are important here. Although termed trap states, the polarons are expected to be mobile because the strong water dipole fluctuations can thermally activate them.

The electrostatic stabilization of the hole due to water polarization is expressed by its contribution to the polaron binding energy $E_{\mathrm{PW}}$,

$$E_{\mathrm{PW}} = \frac{1}{2} \sum_{i \in \mathrm{QM}} \phi_i q_i, \tag{5}$$

where $q_i$ and $\phi_i$ denote the quantum mechanical (QM) charges and the electrostatic potential at carbon site $i$. Note that the factor $\frac{1}{2}$ originates from the assumed linear response of water polarization. Deviations from the ideal linear behavior might occur in the vicinity of polar surfaces such as silicon dioxide or due to ionic impurities. In both cases, the free rotation of water dipoles is hindered with strong consequences on the polaron binding energy. Neglecting these nonlinear effects, Fig. 5 shows the increase in polarization during the first 0.8 ps after the charge was introduced into the pentacene layer for two representative simulations. It can be seen that the energy of the hole is significantly reduced on this time scale although it is strongly modulated by water dipole fluctuations in the liquid phase. From the whole simulation run (0.8 ns), we calculate the average value of the polaron binding energy to be $E_{\mathrm{PW}}=-0.63$ eV. Fluctuations around the average value follow a Gaussian distribution (see inset Fig. 5). Its standard deviation equals the value for the fluctuation of the onsite potentials $\phi_i$ ($\sigma_\phi=0.19$ eV).

The strong polaron binding can be rationalized by continuum electrostatics. The polarization discontinuity at the

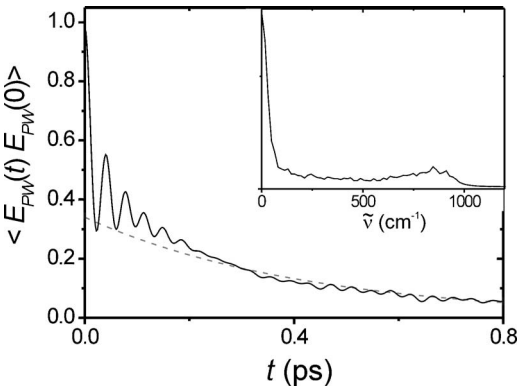


FIG. 6. Autocorrelation function of water-induced fluctuations in the polaron binding energy $E_{\mathrm{PW}}(t)$ and Fourier transform of the fluctuations (inset).

water/pentacene interface in the presence of a hole results in an image force.[44] In the approximation of a large distance $z$, the classical expression for the image potential is written as

$$E_{\mathrm{PW}} = \frac{e^2}{16\pi\varepsilon_0 z}\frac{\varepsilon_W - \varepsilon_P}{\varepsilon_P(\varepsilon_W + \varepsilon_P)}, \tag{6}$$

where $\varepsilon_W$ and $\varepsilon_P$ are the permittivities of water and pentacene. The distance $z$ corresponds to the position of the polaron center and we use $z=6.5$ Å. For the permittivity of the outermost pentacene layer, we assume $\varepsilon_P=1$,[45] for water we use $\varepsilon_W=78$. Equation (6) then results in $E_{\mathrm{PW}}=-0.55$ eV. It is also interesting to notice that the experimental value for the polarization at the gold/pentacene interface[46] is $E_{PM}=-0.67$ eV and thus fits quite well in the image charge interpretation with $\varepsilon_G \to \infty$.

A quantitative analysis of the time scales relevant for the polaron formation can be obtained by the autocorrelation function of the polaron binding energy $\langle E_{\mathrm{PW}}(t)E_{\mathrm{PW}}(0)\rangle$. Figure 6 reveals that the decay in correlation proceeds on two different time scales. A fast vibrational process leads to a fluctuating decay on the time scale of a few femtoseconds. The long-time decay of correlation then shows a roughly exponential form with a time constant of $\tau=0.4$ ps. Both processes can be also identified as peaks in the corresponding spectrum as calculated by the Fourier transformation of the autocorrelation function (Fig. 6 inset). A comparison with the SPCE infrared (IR) spectra shows that the high-frequency librational modes are stronger coupled to the hole charge and the corresponding peak appears in the spectrum at 844 $\mathrm{cm}^{-1}$.[47] Its frequency can be regarded as an upper limit for thermally activated polaron hopping ($k_{0,\max}=2.5\times10^{13}$ $\mathrm{s}^{-1}$).

To investigate hopping processes in our simulation, we follow the center of the positive hole charge. The analysis of the spatial extension of the polaron according to Eq. (4) provides a value for its localization center $\vec{s}_{\mathrm{HOMO}}$ for each snapshot. Figure 7 shows an example for the trajectory of a polaron center over a time interval of 3 ps. The periodic boundary conditions were compensated by unfolding the trajectory. Movements in the two unit-cell directions parallel to the film $a$ and $b$ are regarded separately. It can be seen that

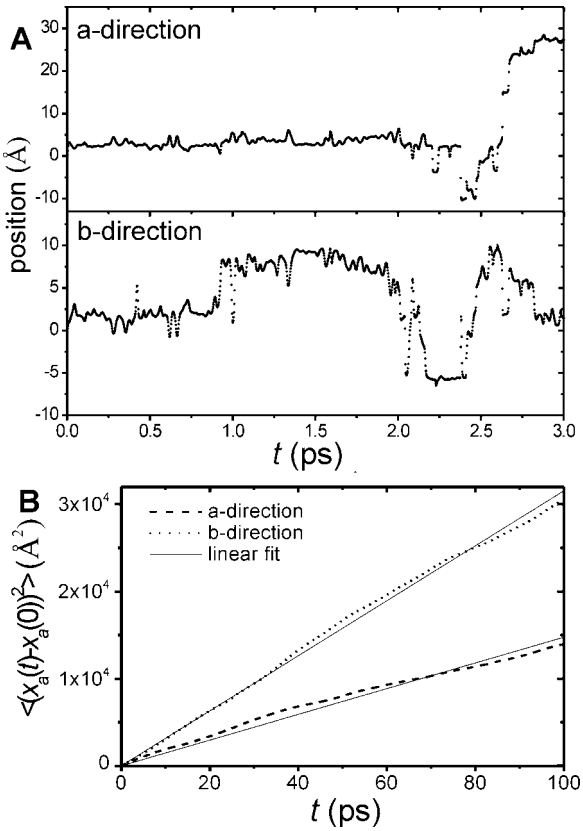


FIG. 7. Polaron diffusion. (a) Plot of an unfolded trajectory of the polaron center along the two crystal directions parallel to the film. At $t=0$ the center of charge is at position $x_a$ and $x_b=0$. (b) The averaged squared displacement in the two crystal directions parallel to the film ($a$ and $b$) is plotted as a function of time. The averaged data are based on a 0.8 ns simulation.

the localization center shows fast fluctuations and from time to time longer nonreversible jumps occur. Even longer distances of up to 10 Å are bridged within a few femtoseconds, in which the localization center shifts constantly between the initial and the final position. For a quantitative study of the charge motion along the pentacene film, we monitored the time dependence of the averaged squared displacement of the polaron center in the two directions $a$ and $b$ [Fig. 7(B)]. After a short initial period (<0.5 ps), the squared displacement increases linearly with time and thus reveals diffusive behavior. The diffusion coefficient can be extracted according to

$$2tD_a = \langle [x_a(t) - x_a(0)]^2 \rangle. \tag{7}$$

As we are here interested in electronic transport, we use the Einstein-Smoluchowski relation to calculate values for the mobility in the field free limit,

$$\mu_a = \frac{eD_a}{k_B T}. \tag{8}$$

From a linear fit we obtain $\mu_a=0.30$ $\mathrm{cm}^2\ \mathrm{s}^{-1}\ \mathrm{V}^{-1}$ and $\mu_b=0.63$ $\mathrm{cm}^2\ \mathrm{s}^{-1}\ \mathrm{V}^{-1}$. The mobility values are close to the upper limit of an incoherent transfer mechanism, where the hopping barriers between localization centers are no longer the rate limiting factors, but—instead—the frequency of the

fluctuations in the electric field determines the rates.[48] The mobility values are also close to the best experimental values measured in pentacene OTFTs.[6] In addition, we observe anisotropic behavior in the mobility, where motion in the *b* direction of the unit cell is faster.

To rationalize these findings, we quantify the spatial extension of the hole. Water polarization induces additional localization of the electronic states. On average, the radius of the polaron $R_G$ is 5.3 Å, which is 0.5 Å less than the unpolarized case (see Table I). Hence the charge contraction due to the nuclear polarization is small compared to the disorder effect. Comparison with the extension of the HOMO state on a single pentacene molecule in vacuum (Table I) shows that the charge is not completely localized on one molecule, as often assumed for pentacene, but instead it extends to the first neighbors of the highest charged pentacene molecule. We find on average a charge of 0.56, 0.23, and 0.09 on the three most charged pentacene molecules. The anisotropy of the crystal structure is reflected in the spatial extension of the hole in the three unit-cell directions *a*, *b*, and *c*. The hole is continuously delocalized along the molecular axis in the *c* direction, independent of the electronic disorder or polarization. In all three cases, the localization parameter $R_{G,c}$ amounts to 3.3 Å. Instead the localization parameters in the direction of the film $R_{G,a}$ and $R_{G,b}$ show stronger variations. We find a reduced charge extension in the *a* direction, which is attributed to the smaller electronic overlap between the pentacene molecules in this direction and is in agreement with the anisotropy observed in band-structure calculations.[24] These findings permit a first interpretation of the simulated mobility values. Although the polaron is centered on one molecular center, nearly 50% of the total charge are smeared out to neighboring pentacene molecules.[49] The magnitude of this effect is determined by the electronic coupling $V_{DA}$ between a pair of pentacene molecules, which is anisotropic due to their orientation in the crystal cell (for a discussion of our calculated $V_{DA}$ values, see below). We conclude that the spatial extension of the polaron and therefore the electronic coupling influence the activation barriers $E_A$ that have to be overcome in the observed hopping transfer.

In incoherent transfer, the height of the hopping barriers is generally controlled by the dielectric surrounding, which here is the water layer. The tunnel splitting $E_t$ at the transition state determines if nonadiabatic processes have to be taken into account and is directly related to the electronic coupling $E_t=2|V_{DA}|$. To quantify $E_A$ and $V_{DA}$ which control the charge transfer between pentacene centers, we investigate the free-energy surface on which polaron hopping occurs. As the number of nuclear degrees of freedom is large, we introduce a simplified reaction coordinate. The underlying idea is that the nuclear degrees of freedom control the electrostatic potential on the pentacene molecules. In addition, the center of the hole charge resides on the molecule with the lowest potential. As an effective reaction coordinate for transfer between a pair of molecules, we define the averaged difference in electrostatic potential,

$$Q_{pq} = \langle \phi_i \rangle_q - \langle \phi_i \rangle_p, \tag{9}$$

where *p* and *q* denote the two pentacene molecules involved in the transfer. The free energy is then calculated according to Boltzmann's equation,

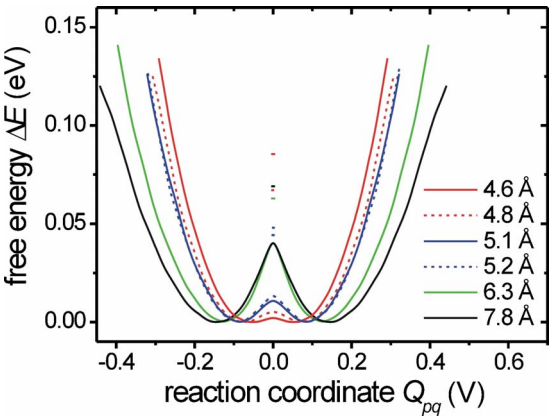


FIG. 8. (Color online) Free-energy profiles for the polaron hopping in a pentacene layer in contact with water. Hopping steps between different pairs of pentacene molecules in the film are considered. The distances between molecular centers are marked (see Table II).

$$\Delta E(Q_{pq}) = -k_B T \ln w(Q_{pq}). \tag{10}$$

The probability $w(Q_{pq})$ to find the system at the position $Q_{pq}$ of the reaction coordinate was extracted from full QM-MM simulations of 0.5 ns. For averaging we used an interval size of 0.015 V. The resulting energy profiles for the six closest pairs of charge transfer [as defined in Fig. 2(B)] are shown in Fig. 8. (We note that for transfer 5 and 6, there are two symmetrically nonequivalent possibilities in the film. However, the electronic couplings are nearly identical and we do not distinguish them in our analysis.) All profiles have the familiar shape of two harmonic potential-energy wells that are separated by a barrier. The calculated values for $E_A$ are listed in Table II. The curvature of the profiles changes only slightly for the different transfers, but the location of the potential minima and heights of the reaction barriers differ between the transfer paths. Decreasing the distance between the molecular centers brings the minima closer together and reduces the barrier. This finding is attributed to spatial correlations in the electrostatic potential $\phi_i$. Changes in $\phi_i$, due to water polarization, occur on the sites where the hole resides and also on neighboring molecules. This correlation

TABLE II. Analysis of the different hopping steps as indicated in Fig. 2. The distance *d* between the molecule centers and the simulated hopping rate *k* are tabulated. Values for the activation barrier $E_A$ and the electronic tunnel splitting $E_t$ stem from an analysis of the free-energy surface.

| Index | *d* (Å) | *k* ($10^{12}$ $s^{-1}$) | $E_A$ (meV) | $E_t$ (meV) | $k_0$ ($10^{12}$ $s^{-1}$) |
|---|---|---|---|---|---|
| 1 | 4.6 | 10.1 | 1.9 | 82.8 | 10.9 |
| 2 | 4.8 | 7.1 | 5.1 | 61.8 | 8.7 |
| 3 | 5.1 | 6.0 | 10.7 | 33.4 | 9.2 |
| 4 | 5.2 | 5.3 | 13.1 | 34.7 | 9.0 |
| 5 | 6.3 | 1.28 | 40.5 | 22.3 | 6.5 |
| 6 | 7.8 | 1.24 | 40.5 | 28.5 | 6.3 |

increases with decreasing distance between charge donor and acceptor. Hence electrostatic potential differences, as used in the reaction coordinate, decrease and the minima in the profile come closer. It has been shown for water that dipole correlations span distances of up to 15 Å and clearly exceed the range of charge-transfer processes considered here.[50] In this fact, we see a second reason for the low reaction barriers. They are much lower than expected from a simple estimation based on the polaron binding energy, where $E_A \sim E_{\mathrm{PW}}/2 - V_{DA} = 0.3$ eV.

The electronic tunnel splitting is given by $E_t = \kappa(\mathrm{HOMO}) - \kappa(\mathrm{HOMO}-1)$, where $\kappa$ denotes the eigenvalues of the tight-binding Hamiltonian at the transition state of the charge transfer. Values for the transfer to the nearest neighbors can be found in Table II. The values are in the range of a few ten millielectronvolts and exceed in most cases the size of the reaction barrier. We conclude that our adiabatic approximation is justified. Our calculated values are roughly a factor of 2 smaller than those predicted b intermediate neglect of differential overlap/screened approximation (INDO/S) or the extended Hückel approach.[24] This renormalization of the transfer integral due to polarization and diagonal disorder is in agreement with the value predicted by Houili *et al.*[44] The clear distance dependence of $E_t$ in our data is rationalized by the electronic overlap that decreases exponentially with distance between atomic-orbital centers. Deviations from this trend are attributed to the mutual orientation of donor and acceptor and the nodal structure of the molecular wave functions.

Finally, we use the calculated activation energies for a comparison with a classical rate expression in the form $k = k_0 \exp(-E_A/k_B T)$. Values for the transfer rate $k$ can be extracted from the simulation when the molecule where most of the hole resides is taken to be the localization center. Whenever this center changes in the course of the simulation, we count a hopping event. The values for $k$ are listed in Table II and are based on a 2 ns trajectory. Transfer to next-nearest neighbors occurs in the simulation but is rare ($\Sigma_{>8\ \text{Å}} k_i = 0.9 \times 10^{12}\ \mathrm{s}^{-1}$) and is neglected here. Using $k$ and $E_A$, we compute the pre-exponential factor $k_0$ which is also tabulated in Table II. Its size is in the range of $k_B T/h$ as predicted by the theory of the activated complex and below the maximum frequency $k_{0,\mathrm{max}}$ of the water dipole fluctuations. Regarding the different transfer paths, a distance dependence of $k_0$ is observed which is attributed to spatial correlations in the dipole fluctuations. A thorough analysis is beyond the scope of the present paper.

## IV. CONCLUSIONS

We presented an atomistic approach to the water-induced charge localization in pentacene films, focusing on the topmost charge transport layer exposed to the liquid. Orientational polarization of the liquid phase is described by a classical force field. Coulomb force couples the water dipoles to the electronic structure of the semiconductor, which is elaborated in the framework of a tight-binding model. The underlying structural model corresponds to a water-filled nanocavity that is in contact with a crystalline pentacene monolayer which contributes to the charge accumulation in an operating FET. Our findings lead to the following experimentally relevant conclusions.

(i) The presence of water induces amorphous band tails in the semiconductor. The parameter $\beta$ that characterizes the exponential decay of the valence band into the band gap is in good agreement with experimental findings.

(ii) Water polarization happens on a fast time scale ($\tau < 0.5$ ps) and eventually leads to a polaronic trap state with an average binding energy of $E_{\mathrm{PW}} = -0.6$ eV. A slightly stronger polaron binding of $E_{\mathrm{PW}} = -0.8$ eV was obtained by Verlaak and Heremans[51] using a more general microelectrostatic model to describe the interaction of a free rotating dipole and a localized hole charge. Interestingly, also experiments for several different organic semiconductors yield similar values as an activation barrier in temperature-dependent bias-stress measurements.[12,52] Therefore, we suggest that water-induced polaronic trap states might be involved. Our result for pentacene can be generalized to other organic semiconductors as the polaron binding energy depends only on water polarization and the spatial extension of the hole charge. The latter is believed to be generally in the range of lattice dimensions, so similar to our observed value of $R_G = 5.0$ Å. As a consequence, large variations in $E_{\mathrm{PW}}$ are not expected for different materials. However, we note that the bias stress happens on a much slower time scale than the processes observed here, and the full interpretation of the phenomenon is still an open task.

(iii) The polaron remains highly mobile in the vicinity of the water layer. We calculated mobilities in the range of 0.6 $\mathrm{cm}^2\ \mathrm{s}^{-1}\ \mathrm{V}^{-1}$ in the $b$ direction and 0.3 $\mathrm{cm}^2\ \mathrm{s}^{-1}\ \mathrm{V}^{-1}$ in the $a$ direction of the pentacene unit cell. This high mobility for an incoherent transfer mechanism is rationalized by the strong correlated fluctuations of the water dipoles. In addition, the lateral delocalization of the polaron over a few pentacene molecules leads to low barriers between donor and acceptor states.

In conclusion, our calculations support the idea that water-filled nanocavities deteriorate the device performance.[53] Charge carriers are trapped in polaronic states at the water semiconductor interface. However, strong dipole fluctuations in the liquid lead to charge mobility via thermally activated hopping in the direction parallel to the interface. This finding is important for the field of biosensors based on OTFTs, where the organic semiconductor is immersed in an aqueous analyte solution. We predict that even in the absence of a capping layer, the incoherent transfer should lead to mobilities that permit sensor operation with reasonable response times and signal intensities. The adsorption of hydrophobic species to the pentacene surface is then expected to abate the mobility due to a reduced electrostatic coupling to the polaronic trap states.

## ACKNOWLEDGMENT

We gratefully acknowledge partial support from EU project BIODOT (Grant No. STRP 032652) and ONR grant N00014-05-1-0457.

[1] D. M. de Leeuw, M. M. J. Simenon, A. R. Brown, and R. E. F. Einerhand, Synth. Met. **87**, 53 (1997).
[2] J. E. Northrup and M. L. Chabinyc, Phys. Rev. B **68**, 041202(R) (2003).
[3] Y. Qiu, Y. Hu, G. Dong, L. Wang, J. Xie, and Y. Ma, Appl. Phys. Lett. **83**, 1644 (2003).
[4] J. T. Mabeck and G. G. Malliaras, Anal. Bioanal. Chem. **384**, 343-353 (2006).
[5] D. M. Goldie and T. J. Dines, J. Phys. D **40**, 982 (2007).
[6] C. D. Dimitrakopoulos and P. R. L. Malenfant, Adv. Mater. (Weinheim, Ger.) **14**, 99 (2002).
[7] M. Pope and C. E. Swenberg, (Oxford University Press, New York, 1999), p. 337.
[8] C. Goldmann, D. J. Gundlach, and B. Batlogg, Appl. Phys. Lett. **88**, 063501 (2006).
[9] Z.-T. Zhu, J. T. Mason, R. Dieckmann, and G. G. Malliaras, Appl. Phys. Lett. **81**, 4643 (2002).
[10] L. Tsetseris and S. T. Pantelides, Phys. Rev. B **75**, 153202 (2007).
[11] S. Wo, B. Wang, H. Zhou, Y. Wang, J. Bessette, R. L. Headrick, A. C. Mayer, G. G. Malliaras, and A. Kazimirov, J. Appl. Phys. **100**, 093504 (2006).
[12] H. L. Gomes, P. Stallinga, M. Cölle, D. M. de Leeuw, and F. Biscarini, Appl. Phys. Lett. **88**, 082101 (2006).
[13] S. Verlaak, S. Steudel, P. Heremans, D. Janssen, and M. S. Deleuze, Phys. Rev. B **68**, 195409 (2003); F. Dinelli, M. Murgia, P. Levy, M. Cavallini, F. Biscarini, and D. M. De Leeuw, Phys. Rev. Lett. **92**, 116802 (2004).
[14] P. Stoliar, E. Bystrenova, M. Facchini, P. Annibale, M.-J. Spijkman, S. Setayesh, D. de Leeuw, and F. Biscarini (unpublished).
[15] R. Ruiz, A. Papadimitratos, A. C. Mayer, and G. G. Malliaras, Adv. Mater. (Weinheim, Ger.) **17**, 1795 (2005).
[16] M. E. Roberts, S. C. B. Mannsfeld, N. Queralto, C. Reese, J. Locklin, W. Knoll, and Z. Bao, Proc. Natl. Acad. Sci. U.S.A. **105**, 12134 (2008).
[17] I. N. Hulea, S. Fratini, H. Xie, C. L. Mulder, N. N. Iossad, G. Rastelli, S. Ciuchi, and A. F. Morpurgo, Nature Mater. **5**, 982 (2006).
[18] T. Holstein, Ann. Phys. **281**, 725 (2000); H. Bottger and V. V. Bryksin, *Hopping Conduction in Solids* (Akademie-Verlag, Berlin, 1985).
[19] E. Conwell, Proc. Natl. Acad. Sci. U.S.A. **102**, 8795 (2005).
[20] W. P. Su, J. R. Schrieffer, and A. J. Heeger, Phys. Rev. Lett. **42**, 1698 (1979); K. Hannewald and P. A. Bobbert, Appl. Phys. Lett. **85**, 1535 (2004).
[21] N. F. Mott (Clarendon, Oxford, 1979); R. Micnas, J. Ranninger, and S. Robaszkiewicz, Rev. Mod. Phys. **62**, 113 (1990); F. Mancini, M. Marinaro, and H. Matsumoto, Int. J. Mod. Phys. B **10**, 1717 (1996); T. Koslowski, Z. Phys. Chem. **215**, 1625 (2000); N. Utz and T. Koslowski, Chem. Phys. **282**, 389 (2002).
[22] M. Rateitzak and T. Koslowski, Chem. Phys. Lett. **377**, 455 (2003).
[23] C. C. Mattheus, A. B. Dros, J. Baas, A. Meetsma, J. L. de Boer, and T. T. M. Palstra, Acta Crystallogr., Sect. C: Cryst. Struct. Commun. **57**, 939 (2001).
[24] A. Troisi and G. Orlandi, J. Phys. Chem. B **109**, 1849 (2005); R. C. Haddon, X. Chi, M. E. Itkis, J. E. Anthony, D. L. Eaton, T. Siegrist, C. C. Mattheus, and T. T. M. Palstra, *ibid.* **106**, 8288 (2002).
[25] H. J. C. Berendsen, J. R. Grigera, and T. P. Straatsma, J. Phys. Chem. **91**, 6269 (1987).
[26] P. Höchtl, S. Boresch, W. Bitomsky, and O. Steinhauser, J. Chem. Phys. **109**, 4927 (1998); C. Vega and E. de Miguel, *ibid.* **126**, 154707 (2007).
[27] J. W. Ponder and D. A. Case, Adv. Protein Chem. **66**, 27 (2003).
[28] W. A. Harrison, *Electronic Structure and the Properties of Solids* (Dover, New York, 1989).
[29] T. Cramer, S. Krapf, and T. Koslowski, J. Phys. Chem. B **108**, 11812 (2004).
[30] A. Troisi and G. Orlandi, Phys. Rev. Lett. **96**, 086601 (2006).
[31] N. E. Gruhn, D. A. da Silva Filho, T. G. Bill, M. Malagoli, V. Coropceanu, A. Kahn, and J.-L. Bredas, J. Am. Chem. Soc. **124**, 7918 (2002).
[32] Note that the stacked geometry of the pentacene and the hydrogen atoms keep the closest water molecules at distances of greater than 3.5 Å to the atomic-orbital centers. Thus, close range corrections to the Coulomb potential as applied in the former work are negligible.
[33] T. A. Darden, D. York, and L. G. Pedersen, J. Chem. Phys. **98**, 10089 (1993).
[34] D. A. Case, T. E. Cheatham III, T. Darden, H. Gohlke, R. Luo, K. M. Merz, A. Onufriev, C. Simmerling, B. Wang, and R. Woods, J. Comput. Chem. **26**, 1668 (2005).
[35] J. P. Ryckaert, G. Ciccotti, and H. J. Berendsen, J. Comput. Phys. **23**, 327 (1977).
[36] H. Kakuta, T. Hirahara, I. Matsuda, T. Nagao, S. Hasegawa, N. Ueno, and K. Sakamoto, Phys. Rev. Lett. **98**, 247601 (2007); J. Lee, D. K. Hwang, C. H. Park, S. S. Kim, and S. Im, Thin Solid Films **12-15**, 451 (2004).
[37] D. Nabok, P. Puschnig, C. Ambrosch-Draxl, O. Werzer, R. Resel, and Detlef-M. Smilgies, Phys. Rev. B **76**, 235322 (2007).
[38] D. E. Logan and F. Siringo, J. Phys.: Condens. Matter **4**, 3695 (1992).
[39] T. Koslowski, W. Kob, and K. Vollmayr, Phys. Rev. B **56**, 9469 (1997); T. Koslowski and D. E. Logan, J. Phys. Chem. **98**, 9146 (1994).
[40] D. V. Lang, X. Chi, T. Siegrist, A. M. Sergent, and A. P. Ramirez, Phys. Rev. Lett. **93**, 086802 (2004).
[41] C. M. Soukoulis, M. H. Cohen, and E. N. Economou, Phys. Rev. Lett. **53**, 616 (1984); S. R. Elliot, *Physics of Amorphous Materials* (Longman, London, 1990).
[42] J. Mort and J. Knights, Nature (London) **290**, 659 (1981).
[43] P. W. Anderson, Phys. Rev. **109**, 1492 (1958).
[44] H. Houili, J. D. Picon, L. Zuppiroli, and M. N. Bussac, J. Appl. Phys. **100**, 023702 (2006).
[45] Please note that a strong electronic polarization of neutral pentacene molecules corresponds to $\varepsilon_P > 1$. As a consequence, the polaron is shielded from the water, the image charge effect gets smaller, and the polaron binding energy is reduced.
[46] F. Amy, C. Chan, and A. Kahn, Org. Electron. **6**, 85 (2005).
[47] J. Marti, E. Gardia, and J. A. Padro, J. Chem. Phys. **101**, 10883 (1994).
[48] M. H. Cohen, J. Non-Cryst. Solids **4**, 391 (1970).
[49] The neglect of the electronic polarization of neutral pentacene molecules might have two opposing consequences on the polaron localization. On one hand, it induces directly the localiza-

tion of the hole charge. On the other hand, it shields the polaron from the water dipoles and thus reduces diagonal disorder with stronger delocalization as a consequence.

[50] G. Mathias and P. Tavan, J. Chem. Phys. **120**, 4393 (2004).

[51] S. Verlaak and P. Heremans, Phys. Rev. B **75**, 115127 (2007).

[52] S. G. J. Mathijssen, M. Cölle, H. L. Gomes, E. C. P. Smits, B. de Boer, I. McCulloch, P. A. Bobbert, and D. M. de Leeuw, Adv. Mater. (Weinheim, Ger.) **19**, 2785 (2007).

[53] D. Li, E.-J. Borkent, R. Nortrup, H. Moon, H. Katz, and Z. Bao, Appl. Phys. Lett. **86**, 042105 (2005).